



# Identification of EloR (Spr1851) as a regulator of cell elongation in *Streptococcus pneumoniae*

Gro Anita Stamsås,<sup>†</sup> Daniel Straume,<sup>†</sup>  
Anja Ruud Winther, Morten Kjos ,  
Cyril Alexander Frantzen and  
Leiv Sigve Håvarstein \*

Faculty of Chemistry, Biotechnology and Food  
Science, Norwegian University of Life Sciences,  
NO-1432, Ås, Norway.

## Summary

In a screen for mutations suppressing the lethal loss of PBP2b in *Streptococcus pneumoniae* we identified Spr1851 (named EloR), a cytoplasmic protein of unknown function whose inactivation removed the requirement for PBP2b as well as RodA. It follows from this that EloR and the two elongasome proteins must be part of the same functional network. This network also includes StkP, as this serine/threonine kinase phosphorylates EloR on threonine 89 (T89). We found that  $\Delta eloR$  cells, and cells expressing the phosphoablative form of EloR (EloR<sup>T89A</sup>), are significantly shorter than wild-type cells. Furthermore, the phosphomimetic form of EloR (EloR<sup>T89E</sup>) is not tolerated unless the cell in addition acquires a truncated MreC or non-functional RodZ protein. By itself, truncation of MreC as well as inactivation of RodZ gives rise to less elongated cells, demonstrating that the stress exerted by the phosphomimetic form of EloR is relieved by suppressor mutations that reduce or abolish the activity of the elongasome. Of note, it was also found that loss of elongasome activity caused by truncation of MreC elicits increased StkP-mediated phosphorylation of EloR. Together, the results support a model in which phosphorylation of EloR stimulates cell elongation, while dephosphorylation has an inhibitory effect.

## Introduction

The shape of bacteria depends on the shape of their peptidoglycan sacculus. Pneumococci, which are not true cocci, have an ellipsoidal shape that results from a combination of septal and lateral peptidoglycan synthesis. The septal cross-wall is synthesized by the divisome, while peripheral cell-wall elongation is carried out by the elongasome. It is not known whether pneumococcal cells alternate between septal and lateral peptidoglycan synthesis, or if these processes take place simultaneously. Whatever the case, both activities must be strictly regulated and coordinated (Zapun *et al.*, 2008; Philippe *et al.*, 2014).

The peptidoglycan sacculus consists of glycan chains of alternating  $\beta$ -1–4-linked *N*-acetylmuramic acid and *N*-acetylglucosamine cross-linked by short peptides (Vollmer *et al.*, 2008). The synthesis of this gigantic macromolecule involves the penicillin-binding proteins (PBPs). Pneumococci produce six different PBPs: three class A PBPs (PBP1a, PBP1b and PBP2a), two class B PBPs (PBP2x and PBP2b), and the D,D-carboxypeptidase PBP3. Class A PBPs are bifunctional, that is, they catalyze both polymerization of glycan chains (transglycosylation) and cross-linking of stem peptides (transpeptidation) during peptidoglycan synthesis. Class B PBPs, on the other hand, are monofunctional transpeptidases that catalyze the formation of peptide cross-links between adjacent glycan strands (Sauvage *et al.*, 2008; Zapun *et al.*, 2008). PBP3 removes the terminal D-alanine from the pentapeptide side chain, presumably to control the extent of peptidoglycan cross-linking (Hakenbeck and Kohiyama, 1982). The class A enzymes are individually dispensible, but a PBP1a/PBP2a double deletion is lethal. In contrast, PBP2x and PBP2b, which are key component of the divisome and elongasome, respectively, are both essential (Kell *et al.*, 1993; Berg *et al.*, 2013). Another essential key member of the elongasome, RodA, was recently identified as a peptidoglycan polymerase (Meeske *et al.*, 2016). Thus, RodA and PBP2b work together to synthesize the new wall material that is inserted into the lateral cell-wall during cell elongation. In addition to PBP2b and RodA, MreC, MreD, DivIVA, RodZ and CozE have been identified as

Accepted 11 July, 2017. \*For correspondence. E-mail sigve.havarstein@nmbu.no; Tel. +47-67232493; Fax 47-64965901. <sup>†</sup>These authors contributed equally to this work.

important for the normal function of the pneumococcal elongasome (Alyahya *et al.*, 2009; Land and Winkler, 2011; Massidda *et al.*, 2013; Philippe *et al.*, 2014; Fenton *et al.*, 2016; Straume *et al.*, 2017).

Several studies have reported that the eukaryotic-type Ser/Thr protein kinase, StkP, is a key regulator of pneumococcal cell-wall synthesis and cell division (Beilharz *et al.*, 2012; Fleurie *et al.*, 2012; Morlot *et al.*, 2013; Fleurie *et al.*, 2014b; Manuse *et al.*, 2016). Deletion of StkP results in morphological alterations, increased susceptibility to environmental stresses and reduced virulence and transformability (Echenique *et al.*, 2004; Beilharz *et al.*, 2012; Fleurie *et al.*, 2012). StkP is a bitopic membrane protein. The extracellular part consists of four PASTA domains, while the intracellular part is composed of a flexible approximately 65 amino acid juxtamembrane domain of unknown function and a kinase domain (Morlot *et al.*, 2013; Manuse *et al.*, 2016). Presumably, the PASTA domains detect specific external signals, which are relayed to intracellular effector proteins through activation of the kinase domain. PASTA domains have been shown to bind peptidoglycan fragments and  $\beta$ -lactams (Shah *et al.*, 2008; Maestro *et al.*, 2011; Mir *et al.*, 2011). It is, therefore, possible that the PASTA domains of StkP modulate its kinase activity by recognizing specific substructures in the peptidoglycan layer. Moreover, very recently, compelling evidence that the cell wall precursor lipid II acts as signal for StkP have been reported (Hardt *et al.*, 2017). The PASTA domains are also responsible for targeting StkP to the septal region, perhaps by recognizing unlinked peptidoglycan (Beilharz *et al.*, 2012; Manuse *et al.*, 2016; Grangeasse, 2016). *stkP* is co-transcribed with the phosphatase *phpP*, which specifically dephosphorylates StkP and StkP target proteins. Hence, the two enzymes operate as a functional couple (Nováková *et al.*, 2005; Ulrych *et al.*, 2016).

To fully understand the biological role of StkP, the phosphorylation targets of StkP must be identified and their functions characterized. StkP-targets reported to be involved in peptidoglycan synthesis or cell division/elongation include MurC, GlmM, MapZ (LocZ), DivIVA, FtsZ and FtsA (Nováková *et al.*, 2005; Sun *et al.*, 2010; Falk and Weisblum, 2012; Fleurie *et al.*, 2014a; Holecková *et al.*, 2015). Phosphoproteomic analysis has identified more than 80 phosphoproteins in *S. pneumoniae* (Sun *et al.*, 2010). It is therefore likely that a number of StkP phosphorylation targets remain to be identified and characterized. One poorly characterized protein targeted by StkP is Spr1851. It belongs to a family of proteins termed Jag (*jag = spoIIIJ* associated gene) (Errington *et al.*, 1992; Sun *et al.*, 2010; Ulrych *et al.*, 2016). Jag homologs are widespread among Gram-positive bacteria, but their function remains

unknown. In the present study we show that Spr1851 plays an important role in the regulation of cell elongation in *S. pneumoniae*.

## Results

### *Deletion of spr1851 enables pneumococci to survive without a functional elongasome*

PBP2b and RodA are both essential and constitute the core components of the elongasome. Previously, we have observed that PBP2b-depleted pneumococci display distinct phenotypic traits. They form long chains of oblate cells, get an altered stem peptide composition, lose immunity to the peptidoglycan hydrolase CbpD during competence and become hypersensitive to the autolysin LytA during exponential growth phase (Berg *et al.*, 2013; Straume *et al.*, 2017). Based on these findings, we speculated that the lethality of a *pbp2b* null mutation might be due to LytA-mediated autolysis, and that  $\Delta pbp2b$  mutants would be viable in a  $\Delta lytA$  background. Attempts to replace the *pbp2b* gene with the kanamycin selectable Janus cassette in *lytA*<sup>+</sup> and *lytA*<sup>-</sup> backgrounds gave no colonies on the selection plates after overnight incubation at 37°C, but a few *lytA*<sup>+</sup> as well as *lytA*<sup>-</sup> colonies appeared after 24–144 hours. This shows that PBP2b is essential also in cells lacking LytA. We picked six colonies, designated GS1–6, which were subjected to whole genome sequencing in order to locate possible suppressor mutations. Three of the isolates harboured mutations in the gene encoding the lytic transglycosylase MltG (Spr1370) (Yunck *et al.*, 2016). The GS5 strain expressed a truncated form of MltG ( $\Delta$ aa 169–551), while the GS1 and GS2 strains produced MltG proteins with amino acid substitutions at their C-terminal ends. GS1-MltG contained only an A505V substitution, while GS2-MltG contained 16 amino acid substitutions between I477 and A505. Shortly after we had made this discovery, Tsui *et al.* (2016) published the same finding, that is, that deletion of *mltG* removes the requirement for PBP2b.

We, therefore, chose to focus on another possible  $\Delta pbp2b$  suppressor mutation identified in the whole-genome sequence analysis. The remaining isolates, GS3, GS4 and GS6, contained mutations in a gene (*spr1851*) encoding a protein of unknown function which is conserved among Gram-positive bacteria. The mutations resulted in truncations of the predicted protein products (Fig. 1A, see Supporting Information Fig. S1 for details). To verify that a non-functional *spr1851* gene is able to suppress the loss of *pbp2b*, we first replaced the complete *spr1851* gene with the Janus cassette in our wild-type strain RH425. The resulting  $\Delta spr1851$  mutant showed marked growth defect compared with

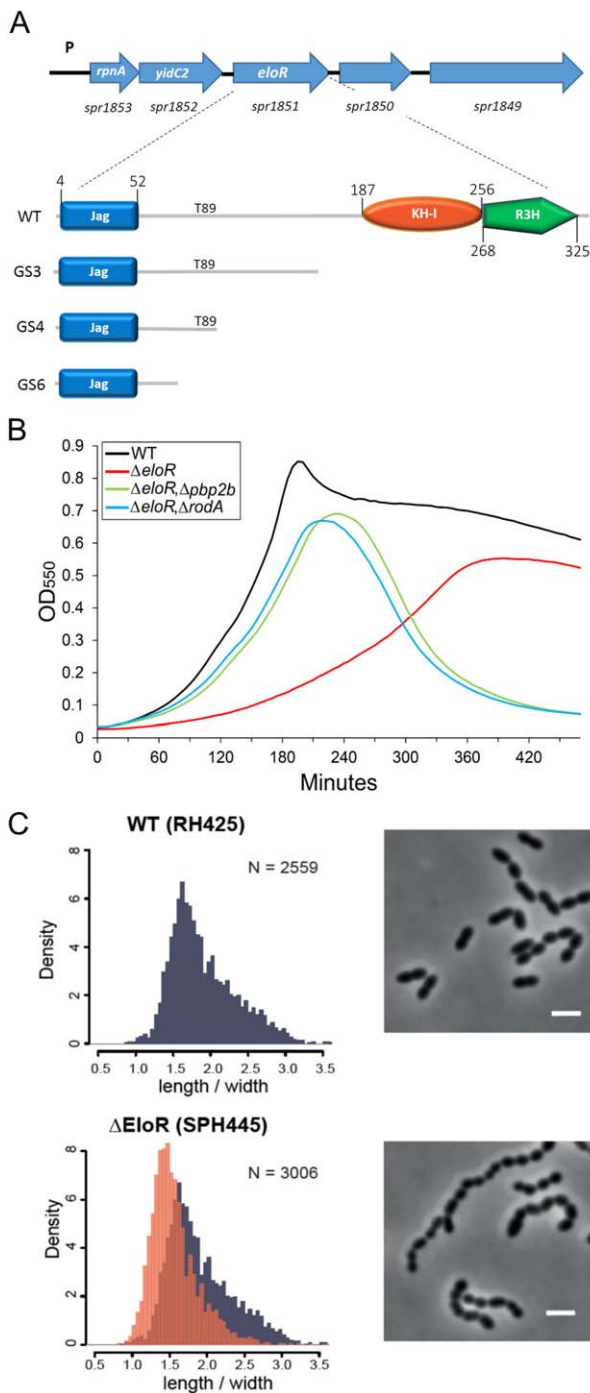


**Fig. 1.** Properties of a  $\Delta eloR$  strain with respect to growth rate, cell shape distribution and morphology. Panel A. Genetic map of the *S. pneumoniae* genome region where *eloR* is located. The ELoR protein consists of 328 amino acids, and is composed of an N-terminal Jag domain and two single-strand nucleic acid binding domains, KH-I and R3H, at the C-terminal end. The position of threonine 89, which is phosphorylated by StkP, and the positions of the domain boundaries are indicated. The truncated forms of ELoR expressed by the suppressor mutants GS3, GS4 and GS6 are shown as schematic drawings. Panel B. Comparison of the growth rates of the SPH445 ( $\Delta eloR$ ) and RH425 (WT) strains. The reduction in growth rate caused by deletion of *eloR* is nearly abolished in strains where *pbp2b* or *rodA* (strains SPH446 and SPH447 respectively) are deleted in addition to *eloR*. Panel C. Comparison of cell shape distribution (length/width ratios) and morphology of the SPH445 ( $\Delta eloR$ ) and RH425 (WT) strains. The histogram representing the shape distribution of wild-type cells (RH425) is shown in grey, while the histogram representing the  $\Delta eloR$  mutant strain (SPH445) is shown in orange. The number of cells counted are indicated for each plot. The length/width ratio of  $\Delta eloR$  cells ( $1.56 \pm 0.33$ ) was significantly different from WT ( $1.91 \pm 0.45$ ) ( $P < 0.01$ , Kolmogorov–Smirnov test). Scale bars in the phase-contrast images represent  $2 \mu\text{m}$ .

transformed at a normal frequency. A few colonies were picked and cultivated in liquid media for further analysis. The absence of the genes encoding Spr1851 and PBP2b in these transformants was confirmed by PCR as well as Sanger sequencing. In addition, the absence of PBP2b in one of them (SPH446) was verified by staining with Bocillin FL, a fluorescent penicillin that specifically labels PBPs (see Materials and Methods and Supporting Information Fig. S2).

Similar to PBP2b, RodA is essential in *S. pneumoniae* (Meeske *et al.*, 2016; Straume *et al.*, 2017). Due to the close functional relationship of these proteins, we speculated that both might be dispensable in a  $\Delta spr1851$  background. We therefore attempted to delete the *rodA* gene in a strain lacking the *spr1851* gene. Interestingly, we succeeded in obtaining transformants that upon further characterization proved to be *bona fide rodA* deletion mutants (e.g., SPH447). Notably, the growth defect observed for the  $\Delta spr1851$  strain is partially alleviated in the  $\Delta spr1851/\Delta pbp2b$  and  $\Delta spr1851/\Delta rodA$  double mutants (Fig. 1B). Together, these results show that pneumococci are not only able to survive without PBP2b or RodA in a  $\Delta spr1851$  background, but the presence of these proteins are detrimental when Spr1851 is absent.

wild-type (Fig. 1B). Next, the Janus cassette was removed by negative selection (Sung *et al.*, 2001), giving rise to the SPH445 mutant strain (see Supporting Information Table S1 for list of strains). SPH445 and the wild-type RH425 strain were transformed with the  $\Delta pbp2b$ -amplicon described above. As expected, no transformants were obtained with the wild-type strain. The mutant strain lacking *spr1851*, however, was

#### *Spr1851 is involved in the regulation of cell elongation in S. pneumoniae*

Spr1851 contains three regions with strong homology to previously described domains, namely Jag ( $\sim 50$  aa), KH-I ( $\sim 76$  aa) and R3H ( $\sim 61$  aa) (Fig. 1A). The C-terminal KH-I and R3H domains are both known to bind ssRNA or ssDNA, and are typically found in proteins

regulating gene expression (Grishin, 1998; Valverde *et al.*, 2008; Jaudzems *et al.*, 2012). The function of the N-terminal JAG domain, on the other hand, remains unknown. Considering that Spr1851 contains KH-I and R3H domains, resides in the cytoplasm, and when absent suppresses the requirement for PBP2b and RodA, it is highly likely that Spr1851 functions to regulate the activity of the elongasome. To further corroborate this theory we used the image analysis tool MicrobeJ (Ducret *et al.*, 2016) to compare the cell shape distribution (length/width ratio) of the SPH445 ( $\Delta spr1851$ ) and RH425 (WT) strains. The results showed that  $\Delta spr1851$  mutant cells on average are significantly less elongated than wild-type cells (Fig. 1C), demonstrating that the elongasome is less active in the absence of Spr1851. Hence, we concluded that Spr1851 is involved in regulating the activity of the elongasome and named the protein EloR (elongasome regulating protein). Furthermore, to gain insight into the subcellular localization of EloR we made a C-terminal fusion to monomeric superfolder GFP, and expressed the EloR-m(sf)gfp fusion from an ectopic locus in strain RH425 as well as in the encapsulated *S. pneumoniae* D39 strain. This showed that EloR, similar to other proteins involved in cell elongation in *S. pneumoniae*, localizes to the septal area (Supporting Information Fig. S3).

#### *StkP-mediated phosphorylation of EloR requires functional PASTA domains*

EloR has been shown to be phosphorylated on threonine 89 (Sun *et al.*, 2010; Ulrych *et al.*, 2016). We confirmed this finding by constructing a strain, SPH449, which expresses a phosphoablative (T89A) form of EloR. To be able to immunoprecipitate and detect this mutant protein by Western blotting, a 3xFlag tag was added to its N-terminal end. Similarly, as a positive control, we constructed a strain (SPH448) in which a 3xFlag tag was added to the N-terminal end of wild-type EloR. Furthermore, to determine whether EloR is phosphorylated by StkP, we added a 3xFlag tag to wild-type EloR in a *stkP*<sup>-</sup> strain (SPH450) and a strain (SPH451) expressing the StkP<sup>K42M</sup> mutant protein. In the latter strain, the catalytic lysine residue of StkP (K42) was changed to a methionine, generating a kinase dead protein (Fleurie *et al.*, 2012). The strain (SPH448) expressing the wild-type 3xFlag-EloR protein displayed normal growth, indicating that the Flag tag does not significantly affect the functionality of the EloR protein. To detect phosphorylation of EloR *in vivo*, the Flag tagged proteins were immunoprecipitated with an anti-Flag antibody, followed by Western blotting with an anti-phosphothreonine antibody. Our results verified that

EloR is phosphorylated by StkP on T89 (Sun *et al.*, 2010; Ulrych *et al.* 2016). The anti-phosphothreonine antibody detected two bands of approximately equal intensity in the lane representing wild-type EloR (Fig. 2). As the upper band is missing in the strain expressing the phosphoablative (T89A) form of EloR, the upper band must represent the T89-phosphorylated form (Fig. 2). The lower band and the band detected in strain expressing EloR<sup>T89A</sup> are both absent in the  $\Delta StkP$  strain. Hence, StkP must be able to phosphorylate EloR at two different sites.

The four PASTA domains of StkP are believed to detect extracellular signals that regulate its kinase activity. To determine if the PASTA domains are required for StkP-mediated phosphorylation of EloR, we constructed a strain, SPH452 (StkP <sup>$\Delta$ PASTA</sup>), in which the PASTA domains (amino acids 372–659) were deleted. As demonstrated in Supporting Information Fig. S4, deletion of the PASTA domains does not affect anchoring of the StkP <sup>$\Delta$ PASTA</sup> protein to the cytoplasmic membrane. Our results clearly show that EloR is not phosphorylated in the strain expressing StkP <sup>$\Delta$ PASTA</sup> (Fig. 2), strongly indicating that the phosphorylation state of EloR is regulated by an extracellular signal sensed by the PASTA domains.

Further evidence that EloR is a substrate of StkP was obtained by bacterial two-hybrid analysis. We used the bacterial adenylate cyclase two-hybrid system (BACTH) to test for interactions between EloR and StkP *in vivo*. The system is based on the functional complementation of T18 and T25, two fragments of the catalytic domain of adenylate cyclase from *Bordetella pertussis* (see Materials and Methods for details). Positive interactions

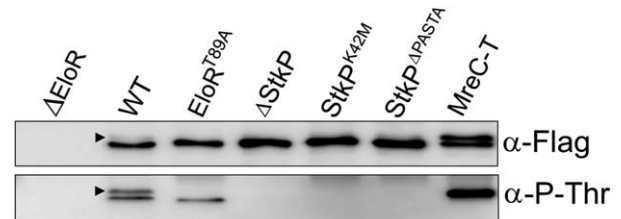


**Fig. 2.** Immunoblot detecting FLAG-tagged EloR with an anti-Flag antibody ( $\alpha$ -Flag) and its phosphorylated form with an anti-phosphothreonine antibody ( $\alpha$ -P-Thr). Lanes were loaded with immunoprecipitates (anti-FLAG antibody conjugated to agarose beads) derived from pneumococcal cell lysates as follows:  $\Delta$ EloR, cells in which the *eloR* gene was deleted; WT, wild-type cells expressing FLAG-tagged EloR; EloR<sup>T89A</sup>, cells expressing the FLAG-tagged phosphoablative form of EloR;  $\Delta$ StkP,  $\Delta$ StkP cells expressing FLAG-tagged EloR; StkP<sup>K42M</sup>, cells expressing both FLAG-tagged EloR and a kinase dead mutant of StkP; StkP <sup>$\Delta$ PASTA</sup>, cells expressing both FLAG-tagged EloR and a version of StkP where the external PASTA domains were deleted; MreC-T, cells expressing both FLAG-tagged EloR and MreC<sup>Aaa183–272</sup>. Arrowheads indicate the position of EloR with a phosphorylated Thr89 residue.

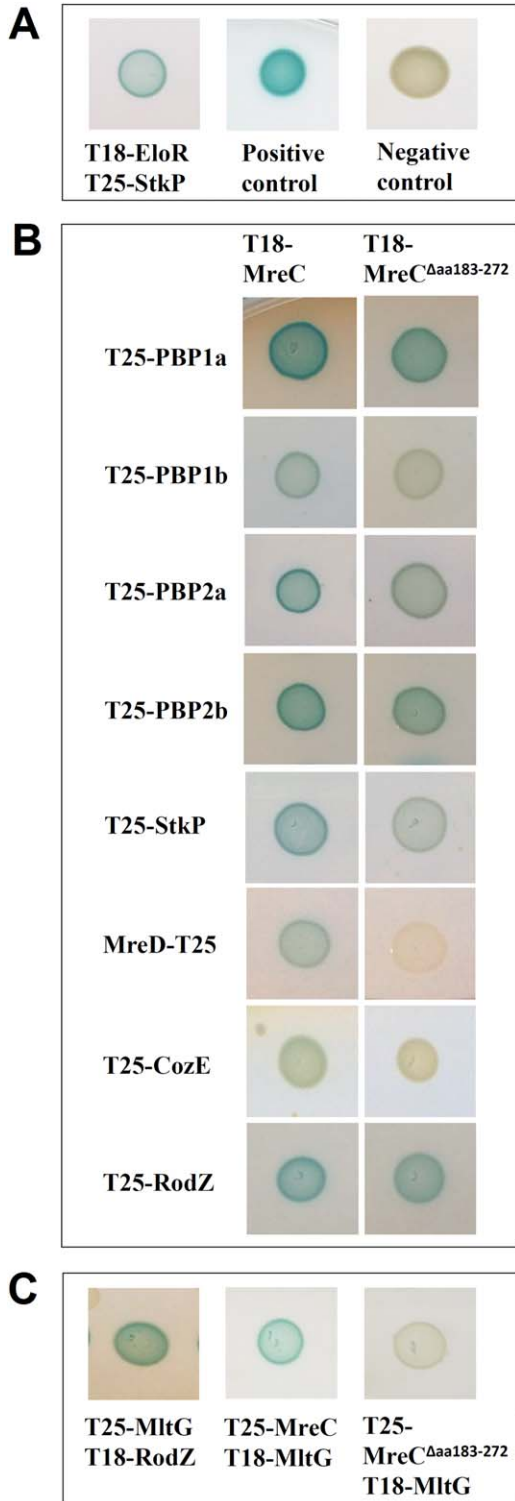


**Fig. 3.** Bacterial two-hybrid data on the interactions between proteins involved in cell elongation. Interactions between pairs of proteins were detected by fusing proteins of interest to adenylate cyclase fragments T18 and T25, respectively, and co-expressing the resulting fusion proteins in an *E. coli cya*<sup>-</sup> strain as specified by the manufacturer (Euromedex). Functional complementation of T18 and T25 fragments restores adenylate cyclase activity resulting in synthesis of cAMP followed by CAP activated expression of  $\beta$ -galactosidase. Samples were spotted on agar plates containing X-gal and incubated for 24 h at 30°C. A colourless spot indicates a negative result, while a blue colour indicates a positive interaction between the pair of fusion proteins tested. Panel A. Interaction between EloR and the Ser/Thr protein kinase StkP. Positive and negative controls were supplied by Euromedex. Panel B. Interactions between full-length and truncated MreC and various elongasome proteins. Panel C. Interactions between the lytic transglycosylase MltG and RodZ, full-length MreC and truncated MreC respectively.

proteins. When co-expressed, the T18-EloR and T25-StkP fusion proteins gave rise to blue colonies, demonstrating that EloR and StkP interact *in vivo* (Fig. 3A).

*The phosphomimetic T89E mutation (EloR<sup>T89E</sup>) is not tolerated*

To gain information about the biological effects of StkP-mediated phosphorylation of EloR, a strain, SPH456, expressing a phosphoablative (T89A) form of EloR was constructed and compared with wild-type (RH425) and the  $\Delta$ EloR mutant (SPH445). In this case, no Flag tag was added to the EloR<sup>T89A</sup> protein. Analysis of their shape distribution showed that the  $\Delta$ EloR and EloR<sup>T89A</sup> strains have highly similar profiles, and that both on average form less elongated cells than the wild-type strain (Fig. 4; Supporting Information Fig. S5). Since deletion of EloR and removal of its phosphorylation site lead to approximately the same reduction in average cell length, it appears that the phosphoablative form of EloR represents a less active or inactive form of the protein. It follows from this that a phosphomimetic (T89E) mutant of EloR might represent the active form that stimulates the activity of the elongasome and increases cell length. To test this hypothesis we constructed an EloR<sup>T89E</sup> mutant strain (SPH457) and analysed it as described above. Unexpectedly, the SPH457 pneumococci were even less elongated than SPH456 cells expressing the EloR<sup>T89A</sup> mutant protein (Fig. 4; Supporting Information Fig. S5). This led us to suspect that the phosphomimetic (T89E) mutation is not tolerated and selects for suppressors. To check for possible suppressor mutations we sequenced the genomes of the SPH445 ( $\Delta$ EloR), SPH456 (EloR<sup>T89A</sup>) and SPH457 (EloR<sup>T89E</sup>) mutant strains, and compared them to the parental strain (RH425). The genomes of the SPH445 and SPH456 strains did not contain suppressors, but a potential suppressor mutation was detected in the

elicited cAMP synthesis followed by cAMP/CAP activated expression of  $\beta$ -galactosidase which converts X-gal to a blue dye. Hence, blue colonies indicate a positive reaction, while white colonies indicate non-interacting

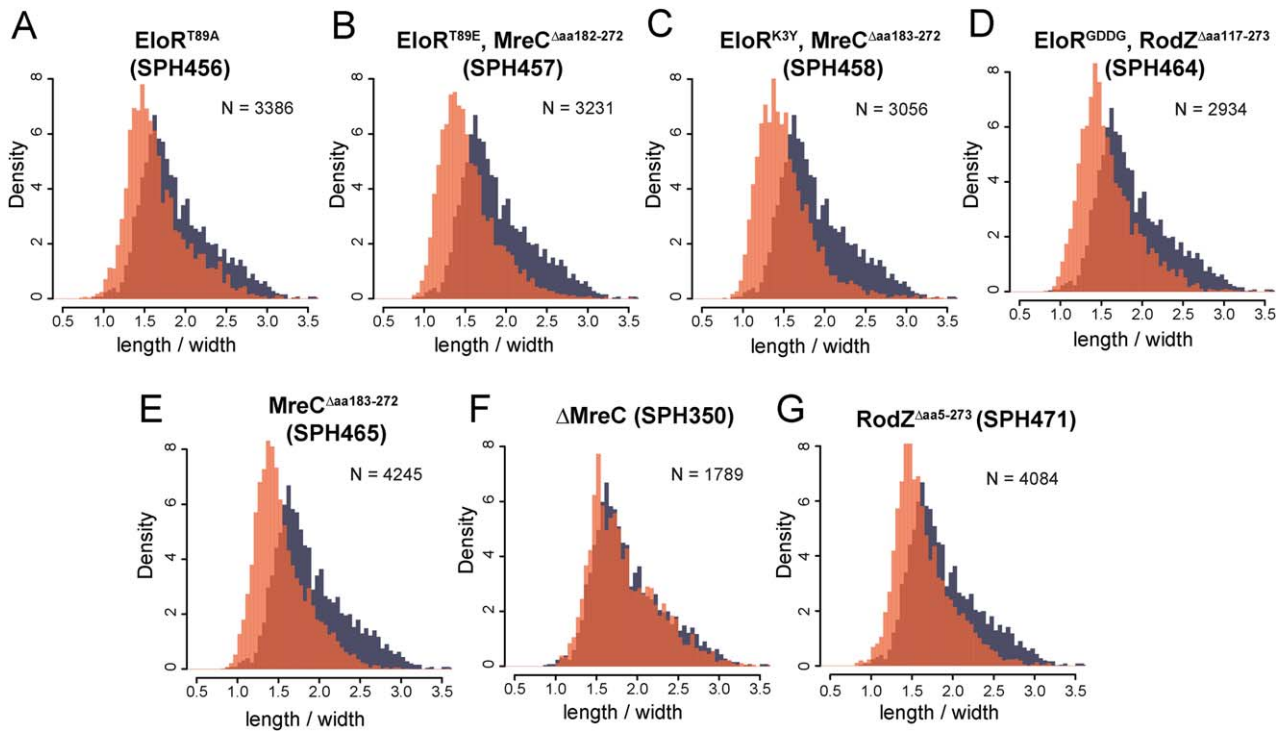


**Fig. 4.** Cell shape distributions. As a measurement for cell elongation, length/width ratio was computed for all counted cells and plotted as histograms (in orange color) for ELoR<sup>T89A</sup> (panel A, length/width ratio  $1.65 \pm 0.37$ ), ELoR<sup>T89E</sup> with suppressor mutation MreC<sup>ΔAaa182-272</sup> (panel B, ratio  $1.53 \pm 0.35$ ), ELoR<sup>K3Y</sup> with suppressor mutation MreC<sup>ΔAaa183-272</sup> (panel C, ratio  $1.52 \pm 0.36$ ), ELoR<sup>GDDG</sup> with suppressor mutation RodZ<sup>ΔAaa117-273</sup> (panel D, ratio  $1.59 \pm 0.36$ ), MreC<sup>ΔAaa183-272</sup> (panel E, ratio  $1.54 \pm 0.34$ ), ΔMreC (panel F, ratio  $1.84 \pm 0.42$ ), RodZ<sup>ΔAaa5-273</sup> (panel G, ratio  $1.64 \pm 0.36$ ). Wild-type RH425 (see Fig. 1C) is shown in grey for all plots for comparison. The length/width ratios of the mutant strains are significantly different from the wild-type ( $P < 0.01$ , Kolmogorov–Smirnov test). Phase contrast microscope images of all strains are shown in Supporting Information Fig. S5A–G. Overlaid density plots length/width ratio distributions for some of the mutants are shown in Supporting Information Fig. S5H. The number of cells counted are indicated for each plot.

genome of the strain expressing ELoR<sup>T89E</sup>. This mutation introduces a frameshift that causes a premature termination of *mreC* mRNA translation, resulting in the synthesis of a truncated protein (MreC<sup>ΔAaa182-272</sup>). Pneumococcal MreC is a bitopic transmembrane protein consisting of 272 amino acids. The N-terminal approximately 8 amino acids are located in the cytoplasm, while the approximately 244 C-terminal amino acids are periplasmic (Lovering and Strynadka, 2007). The amino acid sequence of MreC<sup>ΔAaa182-272</sup> is identical to MreC up to amino acid K181, after which they diverge. Deletion of a single adenosine creates a frameshift that introduces a stop codon 26 amino acids downstream of K181 (see Supporting Information Fig. S6 for details).

Intriguingly, a mutation creating an almost identical truncation of the MreC protein was detected in the genome of a strain (SPH458) expressing an ELoR protein in which the R3H domain was inactivated (ELoR<sup>K3Y</sup>). The R3H domain is characterized by the conserved Arg-X-X-X-His (R3H) sequence motif, where the arginine and histidine residues are required for nucleic acid binding (Grishin, 1998; Jaudzems *et al.*, 2012). In the ELoR<sup>K3Y</sup> mutant strain, the Arg-X-X-X-His sequence was

changed to Lys-X-X-X-Tyr (K3Y). By comparing the genome sequence of the strain expressing ELoR<sup>K3Y</sup> with the parental strain we detected a C to T transition in the *mreC* gene that introduced a premature stop codon after amino acid I182. The resulting truncated MreC protein was termed MreC<sup>ΔAaa183-272</sup>.

The presence of the MreC<sup>ΔAaa182-272</sup> mutation in the strain (SPH457) expressing ELoR<sup>T89E</sup> suggested that the phosphomimetic T89E mutation exerts severe stress that is alleviated by truncation of MreC. To obtain additional evidence in support of this idea, we constructed five new ELoR<sup>T89E</sup> mutants and sequenced their *mreC* genes. In three of the mutants (SPH459–461) we identified the same MreC<sup>ΔAaa183-272</sup> mutation as described above for the SPH458 strain, while two of the mutants (SPH462 and SPH463) had a wild-type *mreC* gene. To determine whether the latter mutant strains had acquired other suppressors, their genomes were sequenced. In both of them a single adenosine was deleted in a run of eight adenosines located 3–10 bases downstream of the translational start codon of the gene encoding RodZ. RodZ is a widely conserved bitopic membrane protein known to play a role in bacterial cell

elongation (Massidda *et al.*, 2013; Philippe *et al.*, 2014). The mutation creates a frameshift that introduces a stop codon eleven codons downstream of the RodZ start site. Hence, it inactivates the protein.

A frameshift mutation in RodZ was also found in a strain in which the KH-I domain of EloR had been mutated (EloR<sup>GDDG</sup>). KH domains contain an invariant GXXG loop in which at least one of the variable amino acids has a positively charged side chain. The loop forms contact with the sugar–phosphate backbone and is crucial for nucleotide binding. It has been reported that mutation of the two variable amino acids to aspartate (GDDG) impairs nucleic acid binding without compromising the stability of the KH domain (Hollingworth *et al.*, 2012). We, therefore, constructed a mutant strain (SPH464) where the native EloR protein was exchanged with a version in which the GYHG loop were mutated to GDDG. Genome sequencing of SPH464 revealed that the five nucleotides TTTAT (nt 330–334) had been deleted in the *rodZ* gene, giving rise to a frameshift after amino acid Y116 (see Supporting Information Fig. S7 for details). The frameshift occurs in the transmembrane segment of the resulting RodZ<sup>Δaa117–273</sup> mutant protein. Thus, while the N-terminal cytoplasmic domain is still expressed, the complete extracellular part is missing. Together, the results described in this section strongly indicate that the phosphomimetic T89E mutation, and mutations that disrupt EloR's ability to bind single stranded nucleic acid, are not tolerated in *S. pneumoniae*.

#### *MreC deletion and truncation mutants have strikingly different phenotypes*

To investigate whether the truncated MreC proteins expressed by the SPH457 (EloR<sup>T89E</sup>/MreC<sup>Δaa182–272</sup>) and SPH458 (EloR<sup>K3Y</sup>/MreC<sup>Δaa183–272</sup>) strains are suppressors that alleviate the stress induced by the EloR<sup>T89E</sup> and EloR<sup>K3Y</sup> mutations, a strain (SPH465) was constructed in which the *mreC* gene of RH425 was replaced by the gene encoding the truncated form of MreC (MreC<sup>Δaa183–272</sup>). As outlined above, the SPH457 and SPH458 strains form on average much less elongated cells than the wild-type strain (Fig. 4; Supporting Information Fig. S5). Comparison of the SHP457, SPH458 and SPH465 strains show that their cell shape distribution is virtually identical, strongly indicating that the MreC<sup>Δaa183–272</sup> mutation rather than the EloR<sup>T89E</sup> or EloR<sup>K3Y</sup> mutations is responsible for the cell rounding observed in the SPH457 and SPH458 strains (Fig. 4; Supporting Information Fig. S5). Comparison of the RH425 (WT) and SPH350 ( $\Delta mreC$ ) strains, on the other hand showed that the shape distribution of their cells is highly similar. Further

characterization of SPH465 (MreC<sup>Δaa183–272</sup>), revealed that the genes encoding PBP2b and RodA can be individually deleted in this strain. Moreover, the growth rates of the SPH465 (MreC<sup>Δaa183–272</sup>) strain, and  $\Delta pbp2b$  or  $\Delta rodA$  mutants of this strain, are similar to wild-type (Supporting Information Fig. S8). These interesting results show that essential components of the elongasome are dispensable in strains expressing the truncated form of the MreC protein (MreC<sup>Δaa183–272</sup>). In contrast, neither *pbp2b* nor *rodA* can be deleted in a wild-type or  $\Delta mreC$  background.

#### *Truncation of MreC alters its interactions with other components of the elongasome and stimulates StkP-mediated phosphorylation of EloR*

MreC has been reported to interact with a number of proteins involved in cell division and elongation (van den Ent *et al.*, 2006). As pneumococci expressing the MreC<sup>Δaa183–272</sup> protein are phenotypically different from wild-type and  $\Delta mreC$  strains, we speculated that truncation of the MreC protein might disrupt its interaction with some partners in the elongasome without disturbing the interaction with others. To test this hypothesis, we used the BACTH system to study interactions between the truncated MreC protein and proteins that we in a previous screening (unpublished results) found to interact with full-length MreC. Strikingly, the results presented in Fig. 3B show that the interaction between MreC and MreD is completely lost when the 90 C-terminal amino acids of MreC are deleted. We also detected a strong reduction in the interaction between MltG and MreC<sup>Δaa183–272</sup> compared with the interaction between MltG and MreC (Fig. 3C). This result was obtained with T18-MltG and T25-MreC. When the adenylate cyclase fragments were swapped (T25-MltG and T18-MreC/T18-MreC<sup>Δaa183–272</sup>), a similar tendency was found although the difference was less evident. In addition, our results suggest that MreC<sup>Δaa183–272</sup> interacts less efficiently with the PBP1b, StkP and CozE proteins than full-length MreC (Fig. 3B). Finally, we made the interesting observation that MltG interacts very strongly with RodZ (Fig. 3C).

As the interaction between MreC<sup>Δaa183–272</sup> and StkP appears to be somewhat reduced compared with the interaction between full-length MreC and StkP, we wondered whether the truncation of MreC might affect StkP-mediated phosphorylation of EloR. To test this possibility, we constructed a strain (SPH475) expressing a 3xFlag-tagged EloR protein and a truncated MreC protein (MreC<sup>Δaa183–272</sup>). To establish the level of EloR phosphorylation in the SPH475 strain, 3xFlag-EloR was immunoprecipitated and subjected to Western blot analysis as described above. Intriguingly, we found that the level of

phosphorylated EloR in this strain was much higher than in a strain expressing full-length MreC (Fig. 2).

## Discussion

We identified EloR by screening for mutations that suppress the lethality caused by deletion of the gene encoding the transpeptidase PBP2b. Subsequent experiments showed that the essential peptidoglycan polymerase RodA is also dispensable in a  $\Delta$ EloR background. These findings demonstrate that pneumococci can survive without a functional elongasome in the absence of EloR. This implies that EloR and the elongasome are part of the same functional network. Although the specific function of EloR remains to be determined, several lines of evidence indicate that it has a regulatory role. Firstly, it contains two regions with strong homology to KH-I and R3H domains. Both domains have been reported to bind single stranded nucleic acid (ssNA) in a sequence-specific manner (Valverde *et al.*, 2008; Hollingworth *et al.*, 2012; Jaudzems *et al.*, 2012). KH domains, which have been more extensively studied than R3H domains, are present in a variety of proteins from all domains of life. They are typically found in proteins that regulate gene expression at the transcriptional or post-transcriptional level (Valverde *et al.*, 2008). Secondly, we found that deletion of EloR significantly reduces the average cell length of the mutant strain compared with wild-type. This demonstrates that EloR is needed to stimulate elongasome-mediated lateral cell wall synthesis. Thirdly, EloR is a substrate of StkP, a transmembrane serine/threonine kinase that is involved in orchestrating the switching between septal and peripheral peptidoglycan synthesis in *S. pneumoniae* through phosphorylation of several proteins involved in cell division and elongation (Nováková *et al.*, 2005; Beilharz *et al.*, 2012; Manuse *et al.*, 2016).

To study the effect of StkP-mediated phosphorylation on T89 we constructed strains expressing the phosphoablative (EloR<sup>T89A</sup>) and phosphomimetic (EloR<sup>T89E</sup>) forms of EloR. The strain SPH456 expressing the phosphoablative form displayed a cell shape profile that was highly similar to that of the SPH445 strain ( $\Delta$ EloR). However, in contrast to the SPH445 strain, the *pbp2b* gene could not be deleted in the SPH456 strain. This shows that the EloR<sup>T89A</sup> protein is not biologically inactive, but its ability to stimulate lateral cell wall synthesis is diminished. Unexpectedly, we observed that EloR<sup>T89A</sup> is still being phosphorylated by StkP (Fig. 2), presumably at a threonine residue located close to T89 at the surface of the protein. Since the  $\Delta$ EloR and EloR<sup>T89A</sup> strains have somewhat different phenotypes, it is likely

that phosphorylation of the alternative site affects the activity of EloR.

The strain expressing the EloR<sup>T89E</sup> phosphomimetic form acquired additional mutations in the *mreC* or *rodZ* gene in all cases examined. Clearly, expression of the EloR<sup>T89E</sup> mutant protein generates stress that is alleviated by truncation of MreC or loss of RodZ function. Truncation of MreC alone resulted in a strong reduction in average cell length, showing that this mutation reduced or inactivated lateral cell wall synthesis (Fig. 4). Similarly, the *rodZ* null mutation present in the SPH462 and SPH463 strains gives rise to less elongated cells (Fig. 4). It follows from this that alleviation of the stress imposed by the phosphomimetic T89E mutation requires suppressor mutations that downregulate or inhibit the activity of the elongasome. In pneumococci expressing truncated MreC (MreC <sup>$\Delta$ Aaa183–272</sup>), loss of elongasome activity is sensed by the cells, which attempt to compensate by strongly increasing StkP-mediated phosphorylation of EloR (Fig. 2). Together these results support a model in which EloR<sup>T89E</sup> and the phosphorylated form of EloR stimulate the activity of the elongasome. Since EloR<sup>T89E</sup> cannot be dephosphorylated by PhpP, but is permanently active throughout the cell cycle, the T89E mutation is probably lethal to the cell. Presumably, the only way to escape the lethality of an overactive elongasome is to acquire suppressors that reduce or abolish the activity of this peptidoglycan synthesizing machine.

Suppressor mutations in the *mreC* or *rodZ* genes were also found in strains expressing EloR proteins containing amino acid substitutions that reduce or abolish their ability to bind ssNA. The SPH458 (EloR<sup>K3Y</sup>) strain acquired the MreC <sup>$\Delta$ Aaa183–272</sup> suppressor mutation, while the RodZ <sup>$\Delta$ Aaa117–276</sup> suppressor was acquired by the strain (SPH464) expressing the EloR<sup>GDDG</sup> mutant protein. Using the same reasoning as above this implies that loss of ssNA-binding activity stimulates the elongasome, while binding of target ssNA probably has an inhibitory effect. As proteins containing ssNA-binding domains are often involved in controlling protein expression by controlling transcription or translation of specific target mRNAs, it is plausible that EloR controls the expression of one or several proteins that are critical for elongasome function. Our data suggest that non-phosphorylated EloR represses target protein expression at the transcriptional or translational level by binding to specific ssDNA or ssRNA sequences. Following phosphorylation of EloR by StkP, the nucleic acid(s) in question is released and target proteins can be synthesized. Further studies are needed to verify or reject this model.

The MreC <sup>$\Delta$ Aaa183–272</sup> mutation gives rise to a distinct and highly interesting phenotype that includes a strong reduction in cell elongation and the ability to grow and proliferate well without PBP2b or RodA. These traits



distinguish the MreC<sup>Δaa183–272</sup> mutant from a ΔMreC strain. Hence, the truncated MreC protein cannot be completely inactive, but must have retained some functions. MreC is an abundant protein present at about 8500 dimers per cell (Land and Winkler, 2011). As mentioned above, the N-terminal approximately 8 amino acids of the bitopic MreC protein is cytoplasmic, while approximately 244 amino acids are located in the periplasm. The periplasmic part of MreC consists of a helix (aa 73–102) and two six-stranded β-barrels (aa 110–272), where the second barrel is folded between strands five and six of the first barrel (van den Ent *et al.*, 2006; Lovering and Strynadka, 2007). The crystal structure shows that MreC dimerizes through close contact between the N-terminal helices. There is also contact between one globular β-barrel from each monomer, while the other β-barrel is solvent exposed and in principle free to interact with another MreC dimer. Hence, it is possible the MreC-dimers are able to form filaments *in vivo* (van den Ent *et al.*, 2006). The truncated MreC<sup>Δaa183–272</sup> protein ends at position 182, which is in the middle of the first β-strand (β6) in the second C-terminal β-barrel. Thus the MreC<sup>Δaa183–272</sup> protein obviously lacks this domain. Since the nine C-terminal amino acids (aa 264–272) form a β-strand (β12) that is part of the first β-barrel, the loss of this strand probably destabilizes the domain and alters its structure. It follows from this that if MreC dimers form filaments, this will not be possible for the MreC<sup>Δaa183–272</sup> protein. It is, therefore, conceivable that loss of filament formation causes or contributes to the phenotype the SPH465 strain.

Since MreC has been reported to bind to a number of different proteins (van den Ent *et al.*, 2006), we investigated whether we could detect any differences between MreC and MreC<sup>Δaa183–272</sup> with respect to protein interaction partners. The most striking result of this study was that the interaction between MreD and MreC was completely lost when the 90 C-terminal amino acids of MreC were deleted (Fig. 3B). The interaction between MreC<sup>Δaa183–272</sup> and PBP1a, PBP2a and PBP2b, on the other hand, was not affected, while the interaction between MreC<sup>Δaa183–272</sup> and PBP1b, StkP and CozE appeared to be somewhat reduced. Based on these results, it is reasonable to assume that the complete loss of interaction between MreC<sup>Δaa183–272</sup> and MreD causes, or significantly contributes to, the distinct phenotype displayed by the SPH465 (MreC<sup>Δaa183–272</sup>) strain. If so, it follows that MreC/MreD interaction is required for activation of elongasome-mediated lateral cell wall synthesis. Curiously, although deletion of MreD causes pneumococci to form long chains of round or oblate cells, *pbp2b* cannot be deleted in these cells (Straume *et al.*, 2017). This shows that loss of the MreC<sup>Δaa183–272</sup>/MreD interaction alone cannot explain all phenotypic differences between

the SPH465 strain and the strains lacking MreC or MreD. It is, therefore, likely that the unique properties of the MreC<sup>Δaa183–272</sup> mutant protein result from the fact that it is no longer able to interact with some MreC partners, while retaining the ability to interact with others (e.g., the PBPs) (Fig. 3B).

In the present study we show that the genes encoding the essential proteins PBP2b and RodA can be readily deleted in a ΔEloR background. Hence, lateral peptidoglycan synthesis per se is not essential for viability in *S. pneumoniae*. So why is deletion of PBP2b and RodA lethal in a wild-type background? The finding that deletion of *mltG* also suppresses the requirement for PBP2b and RodA (Tsui *et al.*, 2016; current study) points toward MltG as the lethal factor. As MltG is an essential muralytic enzyme, misregulation of this enzyme might have fatal consequences. It is conceivable that deletion of PBP2b, RodA and other essential components of the elongasome results in uncontrolled MltG activity that kills the bacterial cells. To gain support for this hypothesis, we tested whether EloR regulates the expression of the MltG protein. Comparison of MltG levels in wild-type (SPH473) and Δ*eloR* (SPH474) cells expressing Flag tagged MltG proteins revealed no significant differences (Supporting Information Fig. S9). Neither is EloR required for septal localization of MltG, as MltG localizes to the septum in wild-type as well as Δ*eloR* cells (Supporting Information Fig. S9). Instead, our results indicate that EloR regulates the muralytic activity of MltG. Presumably, *pbp2b* and *rodA* can be deleted in a Δ*eloR* mutant because the activity of the elongasome, including MltG, is strongly reduced in this genetic background. This supposition is supported by the finding that pneumococcal transformants expressing EloR<sup>T89E</sup> always contain a truncated MreC or nonfunctional RodZ protein. The MreC<sup>Δaa183–272</sup> suppressor mutation strongly reduces the interaction between MreC and MltG, while the Δ*rodZ* suppressor mutation completely abolishes the interaction between RodZ and MltG. Hence, both suppressor mutations probably reduce or modulate the muralytic activity of MltG in a way that helps the cell survive the stress imposed by the phosphomimetic EloR<sup>T89E</sup> mutant protein. The finding that PBP2b and RodA can be deleted in a strain expressing the truncated MreC<sup>Δaa183–272</sup> protein, further supports this model.

In conclusion, our results demonstrate that EloR regulates cell elongation in *S. pneumoniae*. The PASTA domains of StkP sense one or more external signals which are relayed to EloR by transfer of a phosphoryl group. We obtained strong evidence that the phosphorylated form of EloR stimulates cell elongation, while the non-phosphorylated form is less active or inactive. Of note, we observed that strains expressing EloR<sup>T89E</sup> always acquired suppressor mutations that gave rise to

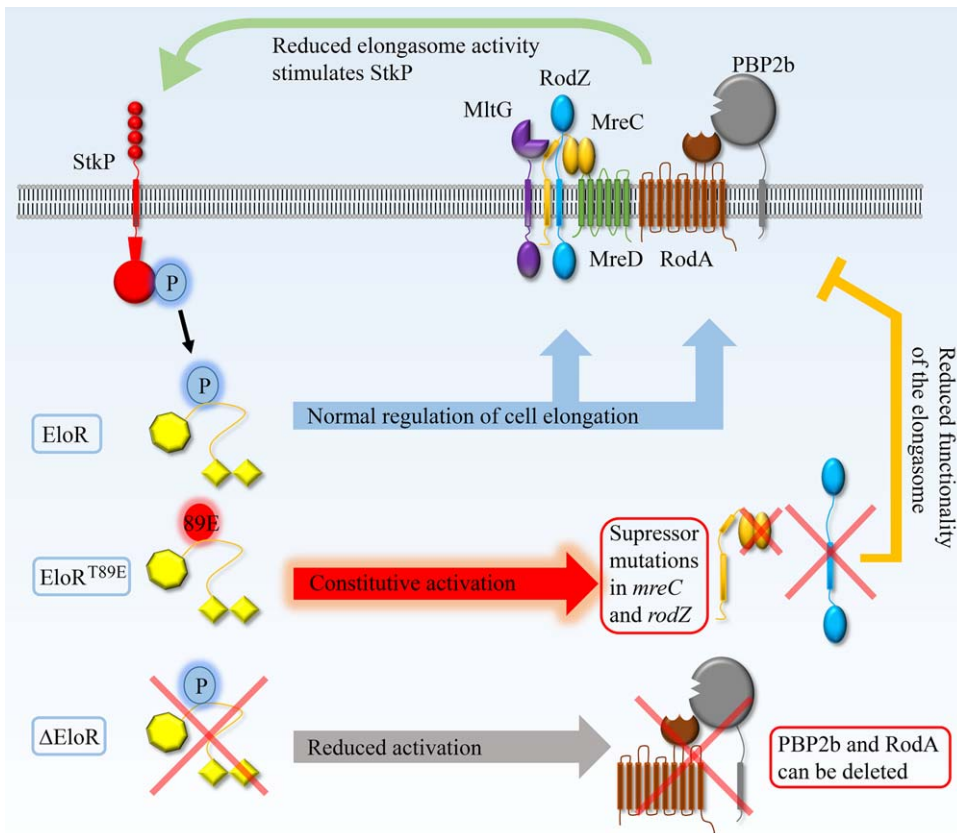


**Fig. 5.** Model depicting ELoR-mediated regulation of the pneumococcal elongasome. At the appropriate stage of the cell cycle, the extracellular PASTA domains of StkP sense an unknown signal linked to elongasome activity that is relayed to ELoR through the transfer of a phosphoryl group. Our results indicate that the phosphorylated form of ELoR activates the elongasome, resulting in synthesis of new peptidoglycan that is inserted into the existing peptidoglycan layer. Cells expressing the phosphomimetic form of ELoR (EloR<sup>T89E</sup>) always acquire suppressor mutations in *mreC* or *rodZ* that strongly reduce elongasome activity. This implies that the suppressors alleviate the stress imposed by a constantly activated elongasome. Deletion of the gene encoding ELoR results in short, rounded, cells that are able to survive without the essential elongasome components PBP2b and RodA.

a less active or inactive elongasome, demonstrating that the constitutively activated phosphomimetic form of ELoR is not tolerated (Fig. 5). Furthermore, the finding that StkP-mediated phosphorylation of ELoR increases strongly in a MreC<sup>Δaa183–272</sup> mutant, suggests that StkP monitors the activity of the elongasome and responds to changes that reduce or abolish its activity (Fig. 5). Several elongasome proteins have been reported to be essential (Massidda *et al.*, 2013; Tsui *et al.*, 2016). Our data suggest that they are not essential by themselves. Instead, we propose that their absence leads to misregulation of the muralytic enzyme MltG, whose unrestrained activity will be lethal to the pneumococcal cell.

## Experimental procedures

### Bacterial strains, cultivation and transformation

Bacterial strains used in this study are listed in the Supporting Information Table S1. Strains of *Escherichia coli* were grown in Luria Bertani broth with shaking or on LB agar plates at 30°C or 37°C. When appropriate, the following antibiotic concentrations were used in the growth medium: ampicillin = 100 µg/ml and kanamycin = 50 µg/ml. Chemically competent *E. coli* was transformed by typical heat-shock at 42°C for 30 seconds. *S. pneumoniae* was grown in C medium (Lacks and Hotchkiss, 1960) at 37°C without

shaking. When selecting for *S. pneumoniae* transformants, the pneumococcus was grown on Todd-Hewitt agar plates in an oxygen-depleted chamber using AnaeroGen™ bags from Oxoid. Gene knockouts or introduction of point mutations in the *S. pneumoniae* genome were performed by natural transformation. Pneumococcal cultures (1 ml) growing exponentially at OD<sub>550</sub> = 0.05–0.1 were mixed with 100–200 ng of the transforming DNA and CSP to a final concentration of 250 ng/ml. After 2 hours of incubation at 37°C, transformants were selected on TH-agar containing the appropriate antibiotic (kanamycin = 400 µg/ml, streptomycin = 200 µg/ml and tetracycline = 1 µg/ml).

When following the growth of *S. pneumoniae* over time, pneumococcal strains were grown in 96-well Corning NBS clear-bottom plates in a Synergy H1 Hybrid Reader (Bio-Tek). First, cells were grown to exponential growth phase (OD<sub>550</sub> = 0.2–0.3) in 5 ml volumes, collected by centrifugation at 4000g and resuspended in fresh C medium to OD<sub>550</sub> = 0.05. Then 300 µl cell culture were transferred to each well of the microtiter plate and incubated in the Synergy H1 Hybrid Reader under normal atmosphere at 37°C. OD<sub>550</sub> was measured automatically every 5 minutes.

### Construction of DNA amplicons

DNA amplicons used to transform *S. pneumoniae* were constructed by overlap extension PCR based on the principle of Higuchi *et al.* (1988). Gene knockouts created in this

study were made by using the Janus cassette (Sung *et al.*, 2001), or in some cases a tetracycline resistance cassette. Basically, approximately 1000 bp flanking regions upstream and downstream of a desired target gene were fused to the 5' and 3' end of the knockout cassette as described in previous works (Johnsborg *et al.*, 2008; Eldholm *et al.*, 2010). By using a streptomycin resistant strain, the Janus cassette can be deleted by replacing it with a DNA fragment containing flanking sequences that are homologous to the corresponding regions flanking the Janus cassette in the genome. Primers used to create DNA amplicons in the present work are listed in the Supporting Information Table S2. All constructs were verified by PCR and Sanger sequencing.

### PBP2b suppressor mutants

Based on our previous work with PBP2b, which showed that cells depleted for PBP2b becomes very sensitive to LytA (Berg *et al.*, 2013), we chose to knock out *pbp2b* in both a LytA<sup>+</sup> and a LytA<sup>-</sup> background. A fragment carrying the Janus cassette fused to the flanking regions of *pbp2b* was transformed into strain RH4 (LytA<sup>+</sup>) and RH6 (LytA<sup>-</sup>) according to standard procedure (see above). After incubating the transformation mixture for 2 hours at 37°C, cells were pelleted, resuspended in 200 µl TH-medium and plated on TH-agar. After 24 hours of incubation at 37°C, three colonies had appeared on the plate containing the LytA<sup>+</sup> strain. PCR confirmed that two of the three transformants were *bona fide*  $\Delta$ *pbp2b* knockouts. Of the two correct  $\Delta$ *pbp2b* mutants, one was genome sequenced and named G1 (Supporting Information Table S1). The plate with the LytA<sup>-</sup> strain also contained 3 colonies after 24 hours of incubation, 5 colonies after 48 hours and approximately 20 new colonies after 6 days of incubation. PCR screening identified five transformants to be *bona fide*  $\Delta$ *pbp2b* mutants (GS2–GS6). Strain GS1–GS6 were genome sequenced to identify possible suppressor mutations.

### Whole genome sequencing

The strains RH425, GS1–GS6, SPH445 and SPH456–SPH464 were grown in 10 ml C medium and collected at 4000g when reaching OD<sub>550</sub> = 0.4. Genomic DNA was isolated by using the NucleoBond® AXG 100 kit from Macherey–Nagel according to the manufacturer's protocol. DNA library was created by using the Nextera XT DNA Library Preparation Kit (Illumina) by following the protocol of the manufacturer, and genome sequencing was done by using an Illumina MiSeq. The RH425 raw sequences were assembled to the reference genome *S. pneumoniae* R6 (NC\_003098.1) using SPAdes v3.10.0 (Bankevich *et al.*, 2012) and annotated using the Prokka pipeline (Seemann, 2014). Genomic analysis of the GS1–GS6, SPH445 and SPH456–464 sequences, including sequence mapping, coverage calculation, variant calling and visualization, was performed using Geneious v8.1.9 (Kearse *et al.*, 2012). Mean sequencing coverage was 50×.

### SDS-PAGE and immunoblotting

To detect Flag-EloR and its phosphorylated form, Flag-EloR was first isolated from a 50 ml cell culture by performing an immunoprecipitation assay using Anti-Flag antibodies conjugated to agarose beads (ANTI-FLAG® M2 Affinity Gel, Sigma). RH425 (WT) and pneumococci expressing Flag-EloR in different genetic backgrounds (SPH448–SPH452) were harvested at OD<sub>550</sub> = 0.3, and auto-lysed in 1 ml of binding buffer (50 mM Tris-HCl [pH = 7.4], 150 mM NaCl, 1 mM EDTA, 1% Triton X-100) by triggering the LytA activity at 37°C for 5 minutes. The lysate was incubated with 40 µl ANTI-FLAG® M2 Affinity Gel at 4°C over-night with gentle mixing. The agarose beads were then washed 3 times in 500 µl TBS (50 mM Tris-HCl [pH = 7.4], 150 mM NaCl) as described by the manufacturer, before 60 µl of SDS-sample buffer was added and the beads were heated to 95°C for 5 minutes. Eight µl samples were separated by SDS-PAGE using a 12% separation gel and the buffer conditions described by Laemmli (1970). The Flag-fused versions of StkP (Flag-StkP, Flag-StkP<sup>K42M</sup>, and Flag-StkP<sup>ΔPASTA</sup>) were detected in the membranes from strain SPH453, SPH454 and SPH455 respectively. Flag-MltG was detected in membranes from strain SPH473 and SPH474. Membranes were isolated from 30 ml cell cultures at OD<sub>550</sub> = 0.3 as described by Straume *et al.* (2017). The membranes were solubilized in 100 µl SDS-sample buffer, and the membrane proteins in 15 µl volumes were separated by SDS-PAGE. A 12% separation gel was used for the MltG fusions and a 10% separation gel for the StkP fusions.

After electrophoresis, the proteins were transferred to a PVDF membrane by electroblotting and both Flag-fused proteins and proteins containing phosphorylated threonines were detected as described previously by Stamsås *et al.* (2017).

### Microscopy techniques and construction of fluorescent fusion proteins

Phase contrast microscopy was used to analyze the morphology of different *S. pneumoniae* mutant strains. Pneumococcal strains were pre-grown to OD<sub>600</sub> = 0.4, then diluted 100-fold and grown to OD<sub>600</sub> = 0.1 prior to microscopy. Cells were spotted directly onto slide with a layer of 1.2% agarose in PBS. Images were acquired using a Zeiss AxioObserver with ZEN Blue software, and an ORCA-Flash 4.0 V2 Digital CMOS camera (Hamamatsu Photonics) using a 100× phase-contrast objective. For cell detection and analysis of cell morphologies, the ImageJ plugin MicrobeJ (Ducret *et al.*, 2016) was used. Data analysis and plotting were performed using RStudio.

The subcellular localization of EloR and MltG was examined by fluorescence microscopy. Strains SPH468 and SPH469 express EloR fused C-terminally to the monomeric superfolder *gfp*, *m(sf)gfp* (Liu *et al.*, 2017) using a Zn<sup>2+</sup> inducible promoter. EloR-*m(sf)gfp* was constructed by ligation of the *eloR* gene into the plasmid pMK17 (van Raaphorst *et al.*, 2017) allowing *eloR* to be fused to *m(sf)gfp* via a flexible, domain breaking linker encoding sequence. The plasmid pMK17 contains homology regions for integration in the non-essential *bgaA* locus of *S. pneumoniae*, and

pMK17-eloR was transformed into *S. pneumoniae* RH425 and D39. The *m(sf)gfp-mltG* fusion was constructed by overlap extension PCR as described above. Strain SPH468, SPH469 and SPH470 pre-grown to  $OD_{600} = 0.4$  were diluted 100-fold and grown for 2 hours prior to imaging. For SPH468 and SPH469, 0.2/0.02 mM  $ZnCl_2/MnCl_2$  was added to the growth medium to induce expression of the fluorescent fusions. Imaging was performed on a Zeiss AxioObserver with the same software, camera and objective as mentioned above. An HXP 120 Illuminator (Zeiss) was used as a fluorescence light source. ImageJ was used to prepare the images for publication.

### BACTH-assay

The BACTH two-hybrid system is based on the complementation of the T18 and T25 domains of the adenylate cyclase derived from *Bordetella pertussis* (Karimova *et al.*, 1998). When the T18 and T25 domains are brought together, it will restore adenylate cyclase activity, leading to the synthesis of cAMP, which in turn results in the expression of  $\beta$ -galactosidase. Proteins of interest are fused to the T18 and T25 domain, co-expressed in a *cya-E. coli* strain, and the  $\beta$ -galactosidase production is detected by growing the cells on LB plates containing X-Gal. A positive interaction between two proteins will result in blue colonies. A negative interaction will appear as white colonies. The BACTH assays were performed as described by the manufacturer (Euromedex). Our genes of interest were cloned in frame with either the T18 or T25 encoding sequences in specific plasmids supplied by the manufacturer, giving rise to either N-terminally or C-terminally T18/T25 fusions. All plasmids used in BACTH analysis are listed in Supporting Information Table S1. The plasmids were first transformed into *E. coli* XL1-Blue cells, from which they were purified. Then, two plasmids, one encoding a T18 fusion and the other encoding a T25 fusion, were co-transformed into *cya-BTH101* cells. Transformants were selected on LB plates containing both ampicillin (100  $\mu$ g/ml) and kanamycin (50  $\mu$ g/ml). Five random colonies were grown in liquid LB at 37°C with shaking. When reaching  $OD_{600} \sim 0.5$ , 2.5  $\mu$ l cell culture were spotted onto LB plates containing ampicillin, kanamycin, 0.5 mM IPTG and 40  $\mu$ g/ml X-gal. The plates were incubated at 30°C overnight. Bacterial spots that appeared blue were regarded as a positive interaction between the two proteins of interest. Each experiment was repeated at least three times.

### Labelling of PBPs with bocillin FL

Fluorescent labelling of PBPs with Bocillin FL was carried according to the protocol of Rutschman *et al.* (2007). Exponentially growing *S. pneumoniae* cells from 10 ml cultures were harvested at 4000g when reaching  $OD_{550} = 0.3$ . The cells were resuspended in 100  $\mu$ l sodium phosphate buffer (20 mM, pH 7.2) with 0.2% Triton X-100. The samples were incubated at 37°C for 5 minutes to allow LytA to completely lyse the cells. The PBPs were fluorescently labelled by adding Bocillin FL to a final concentration of 3.3  $\mu$ M followed by incubation at 37°C for 30 minutes. The labelled PBPs were

separated by SDS-PAGE as described by Rutschman *et al.* and visualized in an Azure C400 imaging system.

### Acknowledgements

The authors would like to thank Zhian Salehian and Dr. Davide Porcellato for excellent technical assistance.

### Author contributions

Conception or design of study: DS, GAS, MK, LSH

Acquisition, analysis or interpretation of data: DS, GAS, ARW, MK, CAF, LSH

Writing of the manuscript: DS, GAS, MK, LSH

### References

- Alyahya, S.A., Alexander, R., Costa, T., Henriques, A.O., Emonet, T., and Jacobs-Wagner, C. (2009) RodZ, a component of the bacterial core morphogenic apparatus. *Proc Natl Acad Sci USA* **106**: 1239–1244.
- Bankevich, A., Nurk, S., Antipov, D., Gurevich, A.A., Dvorkin, M., Kulikov, A.S., *et al.* (2012) SPAdes: a new genome assembly algorithm and its applications to single-cell sequencing. *J Comput Biol* **19**: 455–477.
- Beilharz, K., Nováková, L., Fadda, D., Branny, P., Massidda, O., and Veening, J.W. (2012) Control of cell division in *Streptococcus pneumoniae* by the conserved Ser/Thr protein kinase StkP. *Proc Natl Acad Sci USA* **109**: E905–E913.
- Berg, K.H., Stamsås, G.A., Straume, D., and Håvarstein, L.S. (2013) Effects of low PBP2b levels on cell morphology and peptidoglycan composition in *Streptococcus pneumoniae*. *J Bacteriol* **195**: 4342–4354.
- Ducet, A., Quardokus, E.M., and Brun, Y.V. (2016) MicroBed, a tool for high throughput bacterial cell detection and quantitative analysis. *Nat Microbiol* **1**: 16077.
- Echenique, J., Kadioglu, A., Romao, S., Andrew, P.W., and Trombe, M.C. (2004) Protein serine/threonine kinase StkP positively controls virulence and competence in *Streptococcus pneumoniae*. *Infect Immun* **72**: 2434–2437.
- Eldholm, V., Johnsborg, O., Straume, D., Ohnstad, H.S., Berg, K.H., Hermoso, J.A., and Håvarstein, L.S. (2010) Pneumococcal CbpD is a murein hydrolase that requires a dual cell envelope binding specificity to kill target cells during fratricide. *Mol Microbiol* **76**: 905–917.
- Errington, J., Appleby, L., Daniel, R.A., Goodfellow, H., Partridge, S.R., and Yudkin, M.D. (1992) Structure and function of the *spoIIIJ* gene of *Bacillus subtilis*: a vegetatively expressed gene that is essential for  $\sigma^G$  activity at an intermediate stage of sporulation. *J Gen Microbiol* **138**: 2609–2618.
- Falk, S.P., and Weisblum, B. (2012) Phosphorylation of the *Streptococcus pneumoniae* cell wall biosynthesis enzyme MurC by a eukaryotic-like Ser/Thr kinase. *FEMS Microbiol Lett* **340**: 19–23.

- Fenton, A.K., El Mortaji, L., Lau, D.T.C., Rudner, D.Z., and Bernhardt, T.G. (2016) CozE is a member of the MreCD complex that directs cell elongation in *Streptococcus pneumoniae*. *Nat Microbiol* **2**: 237.
- Fleurie, A., Cluzel, C., Guiral, S., Freton, C., Galisson, F., Zanella-Cleon, I., Di Guilmi, A.M., and Grangeasse, C. (2012) Mutational dissection of the S/T-kinase StkP reveals crucial roles in cell division of *Streptococcus pneumoniae*. *Mol Microbiol* **83**: 746–758.
- Fleurie, A., Lesterlin, C., Manuse, S., Zhao, C., Cluzel, C., Lavergne, J.P., *et al.* (2014a) MapZ marks the division sites and positions FtsZ rings in *Streptococcus pneumoniae*. *Nature* **516**: 259–262.
- Fleurie, A., Manuse, S., Zhao, C., Campo, N., Cluzel, C., Lavergne, J.P., *et al.* (2014b) Interplay of the serine/threonine-kinase StkP and the paralogs DivIVA and GpsB in pneumococcal cell elongation and division. *PLoS Genet* **10**: e1004275.
- Grangeasse, C. (2016) Rewiring the pneumococcal cell cycle with serine/threonine- and tyrosine-kinases. *Trends Microbiol* **24**: 713–724.
- Grishin, N.V. (1998) The R3H motif: a domain that binds single-stranded nucleic acids. *Trends Biochem Sci* **23**: 329–330.
- Hakenbeck, R., and Kohiyama, M. (1982) Purification of penicillin-binding protein 3 from *Streptococcus pneumoniae*. *Eur J Biochem* **127**: 231–236.
- Hardt, P., Engels, I., Rausch, M., Gajdiss, M., Ulm, H., Sass, P., *et al.* (2017) The cell wall precursor lipid II acts as a molecular signal for the Ser/Thr kinase PknB of *Staphylococcus aureus*. *Int J Med Microbiol* **307**: 1–10.
- Higuchi, R., Krummel, B., and Saiki, R.K. (1988) A general method of in vitro preparation and specific mutagenesis of DNA fragments: study of protein and DNA interactions. *Nucleic Acids Res* **16**: 7351–7367.
- Holecková, N., Doubravová, L., Massidda, O., Molle, V., Buriánková, K., Benada, O., *et al.* (2015) LocZ is a new cell division protein involved in proper septum placement in *Streptococcus pneumoniae*. *mBio* **6**: e01700–e01714.
- Hollingworth, D., Candel, A.M., Nicastro, G., Martin, S.R., Briata, P., Gherzi, R., and Ramos, A. (2012) KH domains with impaired nucleic acid binding as a tool for functional analysis. *Nucl Acids Res* **40**: 6873–6886.
- Jaudzems, K., Jia, X., Yagi, H., Zhulenkova, D., Graham, B., Otting, G., and Liepinsh, E. (2012) Structural basis for 5'-end-specific recognition of single-stranded DANN by the R3H domain from human S<sub>μ</sub>bp-2. *J Mol Biol* **424**: 42–53.
- Johnsborg, O., Eldholm, V., Bjørnstad, M.L., and Håvarstein, L.S. (2008) A predatory mechanism dramatically increases the efficiency of lateral gene transfer in *Streptococcus pneumoniae* and related commensal species. *Mol Microbiol* **69**: 245–253.
- Karimova, G., Pidoux, J., Ullmann, A., and Ladant, D. (1998) A bacterial two-hybrid system based on a reconstituted signal transduction pathway. *Proc Natl Acad Sci USA* **95**: 5752–5756.
- Kearse, M., Moir, R., Wilson, A., Stones-Havas, S., Cheung, M., Sturrock, S., *et al.* (2012) Geneious basic: an integrated and extendable desktop software platform for the organization and analysis of sequence data. *Bioinformatics* **28**: 1647–1649.
- Kell, C.M., Sharma, U.K., Dowson, C.G., Town, C., Balganes, T.S., and Spratt, B. (1993) Deletion analysis of the essentiality of penicillin-binding proteins 1A, 2B, and 2X of *Streptococcus pneumoniae*. *FEMS Microbiol Lett* **106**: 171–175.
- Lacks, S., and Hotchkiss, R.D. (1960) A study of the genetic material determining an enzyme in pneumococcus. *Biochem Biophys Acta* **39**: 508–518.
- Laemmli, U.K. (1970) Cleavage of structural proteins during the assembly of the head of bacteriophage T4. *Nature* **227**: 680–685.
- Land, A.D., and Winkler, M.E. (2011) The requirement for pneumococcal MreC and MreD is relieved by inactivation of the gene encoding PBP1a. *J Bacteriol* **193**: 4166–4179.
- Liu, X., Gallay, C., Kjos, M., Domenech, A., Slager, J., van Kessel, S.P., *et al.* (2017) High-throughput CRISPRi phenotyping identifies new essential genes in *Streptococcus pneumoniae*. *Mol Syst Biol* **13**: 931.
- Lovering, A.L., and Strynadka, C.J. (2007) High-resolution structure of the major periplasmic domain from the cell shape-determining filament MreC. *J Mol Biol* **372**: 1034–1044.
- Maestro, B., Nováková, L., Heseck, D., Lee, M., Leyva, E., Mobashery, S., *et al.* (2011) Recognition of peptidoglycan and  $\beta$ -lactam antibiotics by the extracellular domain of the Ser/Thr protein kinase StkP from *Streptococcus pneumoniae*. *FEBS Lett* **585**: 357–363.
- Manuse, S., Fleurie, A., Zucchini, L., Lesterlin, C., and Grangeasse, C. (2016) Role of eukaryotic-like serine/threonine kinases in bacterial cell division and morphogenesis. *FEMS Microbiol Rev* **40**: 41–56.
- Massidda, O., Nováková, L., and Vollmer, W. (2013) From models to pathogens: how much have we learned about *Streptococcus pneumoniae* cell division?. *Environ Microbiol* **15**: 3133–3157.
- Meeske, A.J., Riley, E.P., Robins, W.P., Uehara, T., Mekalanos, J.J., Kahne, D., *et al.* (2016) SEDS proteins are a widespread family of bacterial cell wall polymerases. *Nature* **537**: 634–638.
- Mir, M., Asong, J., Li, X., Cardot, J., Boons, G.J., and Husson, R.N. (2011) The extracytoplasmic domain of the *Mycobacterium tuberculosis* Ser/Thr kinase PknB binds specific muropeptides and is required for PknB localization. *PLoS Pathog* **7**: e1002182.
- Morlot, C., Bayle, L., Jacq, M., Fleurie, A., Tourcier, G., Galisson, F., *et al.* (2013) Interaction of penicillin-binding protein 2x and Ser/Thr protein kinase StkP, two key players in *Streptococcus pneumoniae* R6 morphogenesis. *Mol Microbiol* **90**: 88–102.
- Nováková, L., Sasková, L., Pallová, P., Janecek, J., Novotná, J., Ulrych, A., *et al.* (2005) Characterization of a eukaryotic type serine/threonine protein kinase and protein phosphatase of *Streptococcus pneumoniae* and identification of kinase substrates. *FEBS J* **272**: 1243–1254.
- Philippe, J., Vernet, T., and Zapun, A. (2014) The elongation of ovococci. *Microb Drug Resist* **20**: 215–221.
- Rutschman, J., Maurer, P., and Hakenbeck, R. (2007) Detection of penicillin-binding proteins. In *Molecular Biology of Streptococci*. Hakenbeck, R., and Chhatwal, S. (eds). Norfolk: Horizon Bioscience, pp. 537–542.

- Sauvage, E., Kerff, F., Terrak, M., Ayala, J.A., and Charlier, P. (2008) The penicillin-binding proteins: structure and role in peptidoglycan biosynthesis. *FEMS Microbiol Rev* **32**: 234–258.
- Seemann, T. (2014) Prokka: rapid prokaryotic genome annotation. *Bioinformatics* **30**: 2068–2069.
- Shah, I.M., Laaberki, M.H., Popham, D.L., and Dworkin, J. (2008) A eukaryotic-like Ser/Thr kinase signals bacteria to exit dormancy in response to peptidoglycan fragments. *Cell* **135**: 486–496.
- Stamsås, G.A., Straume, D., Salehian, Z., and Håvarstein, L.S. (2017) Evidence that pneumococcal Walk is regulated by StkP through protein-protein interaction. *Microbiology* **163**: 383–399.
- Straume, D., Stamsås, G.A., Berg, K.H., Salehian, Z., and Håvarstein, L.S. (2017) Identification of pneumococcal proteins that are functionally linked to penicillin-binding protein 2b (PBP2b). *Mol Microbiol* **103**: 99–116.
- Sun, X., Ge, F., Xiao, C.L., Yin, X.F., Ge, R., Zhang, L.H., and He, Q.Y. (2010) Phosphoproteomic analysis reveals the multiple roles of phosphorylation in pathogenic bacterium *Streptococcus pneumoniae*. *J Proteome Res* **9**: 275–282.
- Sung, C.K., Li, H., Claverys, J.P., and Morrison, D.A. (2001) An *rpsL* cassette, Janus, for gene replacement through negative selection in *Streptococcus pneumoniae*. *Appl Environ Microbiol* **67**: 5190–5196.
- Tsui, H.C.T., Zheng, J.J., Magallon, A.N., Ryan, J.D., Yunck, R., Rued, B.E., et al. (2016) Suppression of a deletion mutation in the gene encoding essential PBP2b reveals a new lytic transglycosylase involved in peripheral peptidoglycan synthesis in *Streptococcus pneumoniae* D39. *Mol Microbiol* **100**: 1039–1065.
- Ulrych, A., Holečková, N., Goldová, J., Doubravová, L., Benada, O., Kofroňová, O., et al. (2016) Characterization of pneumococcal Ser/Thr protein phosphatase *phpP* mutant and identification of a novel PhpP substrate, putative RNA binding protein JAG. *BMC Microbiol* **16**: 6.
- Valverde, R., Edwards, L., and Regan, L. (2008) Structure and function of KH domains. *FEBS J* **275**: 2712–2726.
- van den Ent, F., Leaver, M., Bendezu, F., Errington, J., de Boer, P., and Löwe, J. (2006) Dimeric structure of the cell shape protein MreC and its functional implications. *Mol Microbiol* **62**: 1631–1642.
- van Raaphorst, R., Kjos, M., and Veening, J.W. (2017) Chromosome segregation drives division site selection in *Streptococcus pneumoniae*. *Proc Natl Acad Sci U S A*. pii: 201620608. doi: 10.1073/pnas.1620608114.
- Vollmer, W., Blanot, D., and de Pedro, M.A. (2008) Peptidoglycan structure and architecture. *FEMS Microbiol Rev* **32**: 149–167.
- Yunck, R., Cho, H., and Bernhardt, T.G. (2016) Identification of MltG as a potential terminase for peptidoglycan polymerization in bacteria. *Mol Microbiol* **99**: 700–718.
- Zapun, A., Vernet, T., and Pinho, M.G. (2008) The different shapes of cocci. *FEMS Microbiol Rev* **32**: 345–360.

### Supporting information

Additional supporting information may be found in the online version of this article at the publisher's web-site.